Reprinted from "Proceedings of the Fourth Conference on Carbon"
PERGAMON PRESS
OXFORD · LONDON · NEW YORK · PARIS
1960
Printed by The Universities Press, Belfast

CRYSTALLOGRAPHIC AND PHYSICAL CHANGES OF SOME CARBONS UPON OXIDATION AND HEAT TREATMENT*†

W. V. Kotlensky‡ and P. L. Walker, Jr
Department of Fuel Technology, The Pennsylvania State University, University Park, Pennsylvania

(Manuscript received August 19, 1959)

Eleven commercial carbon blacks, one anthracite, and three graphites were studied. Changes in the crystallographic and physical properties upon oxidation and heat treatment were followed by measurements of helium densities, nitrogen low temperature adsorption surface areas (BET), crystallite sizes, and average range of inhomogeneities and surface areas calculated from small-angle X-ray scattering data. On the basis of their change in properties, the carbons can be classified into two main groups. Group one: These carbons show a large decrease in helium density and BET surface area and an increase in particle density upon heat treatment, indicating the production of an extensive closed pore system. Group two: The carbons show an increase in helium and particle densities and a very slight decrease in BET surface area upon heat treatment, indicating the development of a dense, compacted particle structure. The X-ray surface areas and average range of inhomogeneities for the carbons are compared with the BET surface areas and crystallite dimensions, respectively.

1. INTRODUCTION

Carbons are multi-crystalline solids whose properties are affected both by the inherent crystallographic structure of the crystallites and their orientation in the particle. Variations in the crystallographic structure of the carbon crystallite have been thoroughly studied by Franklin[1], Bacon[2], Biscoe and Warren[3], and Bowman[4]. They find that the crystallite size of carbons can range from a low of about 10 Å to thousands of angstrom units in the case of natural graphite. They find that changes in the spacing between carbon basal planes (interlayer spacing) parallel changes in crystallite size. For crystallite sizes of less than *ca.* 150 Å, the interlayer spacing is greater than 3.44 Å. As the crystallite size continues to increase, the interlayer spacing decreases toward a limiting value of 3.3538 Å[1] at 15°C. An interlayer spacing of 3.44 Å is the dividing line between random orientation of carbon basal planes (turbostractic structure) and the advent of some three-dimensional ordering. An interlayer spacing of 3.3538 Å is considered synonymous with complete three-dimensional ordering; intermediate spacings between 3.44 and 3.3538 Å give rise to varying degrees of three-dimensional ordering.

The effect of crystallite size and orientation on the physical properties of carbon have been studied by Dresel and Roberts[5], Lock and Austin[6], Walker and co-workers[7], Walker and Rusinko[8], and Spalaris[9], among others.

* Based on a Ph.D. thesis submitted by W. V. Kotlensky to the Graduate School of the Pennsylvania State University, June, 1959.

† This paper presents the results of one phase of research carried out under Contract No. AT(30-1)-1710, sponsored by the Atomic Energy Commission.

‡ Present address: Jet Propulsion Laboratory, Pasadena, California.

[1] R. E. Franklin, *Acta Cryst.*, **4**, 253 (1951).

[2] G. E. Bacon, *Acta Cryst.*, **3**, 137 (1950).

[3] J. Biscoe and B. E. Warren, *J. Appl. Phys.* **13**, 364 (1942).

[4] J. C. Bowman, *Proc. 1st and 2nd Carbon Conf.*, University of Buffalo (1956), p. 59.

[5] E. M. Dresel and L. E. J. Roberts, *Nature, Lond.* **171**, 170 (1953).

[6] L. D. Lock and A. E. Austin, *Proc. 1st and 2nd Carbon Conf.* University of Buffalo (1956), p. 65.

[7] P. L. Walker, Jr., Frank Rusinko, Jr., J. F. Rakszawski and L. M. Liggett, *Proc. Third Carbon Conf.*, Pergamon Press, (1959), p. 643.

[8] P. L. Walker, Jr. and Frank Rusinko, Jr., *ibid.* p. 633.

[9] C. N. Spalaris, *J. Phys. Chem.* **60**, 1480 (1956).

They all report a substantial closed pore volume in carbon – volume into which helium cannot diffuse within a reasonable period of time at room temperature. Lock and Austin show that the closed-pore volume increases regularly with decreasing crystallite size. They conclude that the closed pore volume is composed of voids between adjacent crystallites, with an average separation between crystallites of 3–8 Å, depending on the type of carbon. Walker and co-workers find that the magnitude of the closed pore volume decreases as crystallite orientation increases for a series of petroleum cokes. They also find that important properties of carbon, such as gas reactivity, coefficient of thermal expansion, electrical resistivity, and tensile breaking strength are affected by crystallite orientation. Some of the above workers[5,8,9] find that the closed pore volume is markedly decreased by small amounts of oxidation of the carbon.

In the present work, crystallographic and physical changes of a wide variety of carbons following heat treatment and oxidation have been studied in detail. The work has had as its main objective a better understanding of the interrelation of the crystallographic and physical structure of carbons. Changes in structure have been followed by a number of standard analytical techniques such as low temperature gas adsorption to determine surface area, helium displacement to determine helium density, X-ray diffraction to determine crystallite sizes and interlayer spacing, and mercury displacement to determine particle density. Changes in particle porosity, both open and closed, are calculated from the X-ray, helium, and particle densities. In addition, much work has been done on perfecting the use of small angle X-ray scattering as an approach helpful to the study of porosity in carbon. In particular, it was of interest to attempt to use small angle X-ray scattering measurements to estimate the closed-pore surface area, since this information cannot be obtained by conventional gas adsorption techniques.

II. EXPERIMENTAL

A. *Physical Measurements*

1. *Helium density apparatus.* The helium densities were determined by the conventional method in which a measured quantity of helium was expanded into a sample of known volume containing a known sample weight. The apparatus (thermostated at 30 ± 0.1°C) was of the constant pressure type; that is, after the expansion of the helium into the sample tube, the pressure was increased to its initial value (*ca.* 500 mm Hg) by decreasing the apparatus volume using mercury displacement. Equilibration time for a run was 1 hr. The minimum precision of the measurements was ±0.03 g/cm³.

2. *Particle density apparatus.* A mercury porosimeter[10], with some minor modifications was used to determine the particle densities. The volume of mercury forced between the particles was followed by the potential drop across a platinum–iridium wire looped and held taut inside a precision bore section of a dilatometer tube. Complete filling of the void volume between particles was taken as the point where a negligible change in potential drop occurred for an increase in pressure. From a knowledge of the weights of sample and mercury and the combined volume of the sample and mercury (with mercury filling all the voids between particles), a particle density could be calculated. The minimum precision of the measurement, where sufficient pressure was available to force mercury into the voids between particles was ±0.08 g/cm³. For some of the smaller particle carbons, mercury could not be forced into the voids between particles at the maximum pressure available; and the particle density had to be estimated, as will be discussed.

3. *X-Ray diffraction apparatus.* A 164° (2θ) General Electric X-ray diffraction unit, XRD-3, was employed to determine interlayer spacings and crystallite sizes of the carbons.

[10] P. L. Walker, Jr., F. Rusinko, Jr. and E. Raats, *J. Phys. Chem.* **59**, 245 (1955).

Nickel-filtered copper radiation was used. The crystallite height and width were determined from the (002) and (10) diffraction peaks, respectively. The interlayer spacings were calculated from the (002) diffraction peak using standard procedures. Samples for X-ray diffraction measurements were prepared by placing about 20 mg of carbon on a microscope slide and mixing with a few drops of collodion and amyl acetate solution. Duplicate samples of each carbon were run. The precision of these measurements for the raw anthracite, ground Ceylon graphite, and carbon blacks was: L_c, ± 2 Å; L_a, ± 6 Å; and d (002), ± 0.04 Å. The precision in d (002) measured for the heat treated anthracite, spectroscopic graphite, and 2μ Ceylon graphite was ± 0.005 Å.

4. *Surface area apparatus.* A standard gas adsorption apparatus[11] was employed to obtain adsorption isotherms, using nitrogen as the adsorbate at 77°K. Specific surface areas, calculated from the isotherms using the BET equation could be duplicated within $\pm 2.5\%$. Samples were prepared for adsorption runs by outgassing under high vacuum at 200°C for at least 10 hr.

5. *Small-angle X-ray scattering apparatus.* The General Electric X-ray diffraction unit, XRD-3, with slight modification was used to obtain the small angle X-ray scattering data. The collimation system consisted of two General Electric 0.01° small-angle scattering slits. Monochromatic copper radiation was obtained by use of a nickel–cobalt balanced filter assembly. A proportional counter served to receive the scattered intensity, which was amplified in a scaler-counting circuit and recorded by a digital printer.

Carbons used in the scattering experiments were dried at least four hours at 100°C. A weight of 0.512 g (found to give the optimum scattering) was compressed into a $\frac{3}{4}$ in. cylindrical slot of a $\frac{1}{8}$ in. thick aluminum slide. A packing pressure of *ca.* 2000 lb/in^2 produced suitable samples. A strip of Mylar previously was fastened over one open side of the slide. The Mylar film aided in holding the sample intact after packing and during the scattering experiments. Scattering from the film was negligible.

Per cent transmission measurements were made on the samples packed for small-angle scattering studies. These measurements served as a check on the packing procedure and as an indication as to whether maximum scattering from the sample would be obtained. A sample that passes 37% of the X-ray beam has been shown to give the most intense scattering[12] of monochromatic radiation, although over the range 32–43% transmission very little change in intensity of scattering is generally observed[13]. The per cent transmission for all samples was found to vary between 30 and 42, except for the original anthracite and original and oxidized ground Ceylon graphite. The transmission for these latter samples varied between 18 and 20%. The high absorption of the radiation by these samples was caused by the high mineral matter content in the anthracite and by the mineral matter content and iron contamination in the ground Ceylon graphite.

As discussed in detail elsewhere[14], considerable effort was expended in aligning the main X-ray beam within a few hundredths of a degree of the true zero prior to conducting small-angle scattering studies. During the operation of the apparatus, a tracing (using a copper–lead stop to reduce intensity) was made of the main beam about every 3 hr, as a check on its position and intensity. If the intensity or position of the main beam differed from previous values, the necessary corrections and adjustments were made[14].

After alignment of the main beam was

[11] P. H. Emmett, *A.S.T.M. Tech. Publ.*, No. 51, 95 (1941).

[12] H. P. Klug and L. E. Alexander, *X-ray Diffraction Procedures for Polycrystalline and Amorphous Materials*, John Wiley, New York (1954).

[13] General Electric X-ray Department, "Small Angle Scattering Slits", Direction 12433.

[14] W. V. Kotlensky, Ph.D. Thesis, The Pennsylvania State University (1959).

completed, a run was made, as briefly described. The sample holder support was rotated 90° in order to allow the main beam to pass through the sample. A Lucite cylinder was placed over the support and rubber tubing fastened to the beam and detector slits. Helium adjusted to a flow rate of 30 cm^3/min was allowed to escape through the two slits, thereby permitting essentially the entire beam length to be enclosed in a low scattering gas. The power source was set at 40 kV and 8 mA. The goniometer was set at 2.000° (2θ) and the micrometer dial adjusted either before or after the zero mark to compensate for the difference between the measured zero mark.

The goniometer was driven at a rate of 1° in 25 min. The scaler and timer was set at a 20 sec interval count and synchronized with the digital printer. These settings resulted in 75 prints per degree. The balanced filter alternatively moved the nickel and cobalt filters in the path of the scattered beam (the change in filters taking place simultaneously with the resetting of the counting circuit and the printing operation).

The printed data were first corrected to monochromatic radiation. This was done by averaging the intensity through the cobalt filter before and after each intensity print through the nickel filter and by subtracting this average value from the intensity print through the nickel filter. Corrections for background scattering were made by subtracting the intensities recorded for the main X-ray beam from the intensities obtained with the sample in place. This correction was unimportant at angles above 0.16° (2θ). Other corrections for polarization, absorption, slit height and width were found to be negligible.*

6. *Description of samples.* A brief description of the carbon blacks, graphites, and anthracite selected for this study, including some physical characteristics supplied by the manufacturer follows:

Carbolac 1, Carbolac 2, Mogul A, and Monarch 71 are Godfrey L. Cabot's channel blacks of varying jetness used primarily as color and ink blacks. They are characterized by an average particle size from 100 to 400 Å and contain from 12 to 17% volatile matter which is primarily oxygen.

Cabot's rubber blacks included in this study are: Spheron 6, a medium processing channel black; Vulcan 3, an oil furnace black; Sterling S, a gas furnace black; Sterling FT, a fine thermal black; and Sterling MT, a medium thermal black. With the exception of Spheron 6, which has a volatile content of 5%, these rubber reinforcing carbon blacks have a volatile matter content of less than 1%. The average particle diameters vary respectively from 300 Å for Spheron 6 to 5600 Å for Sterling MT.

Shawinigan or acetylene black, a product of the Shawinigan Products Corp., is made by the thermal decomposition of acetylene in a continuous process. This carbon black is unusual in that the particles are joined together in a chain-like fashion. The average particle size is 420 Å. The volatile content is less than 1% and is essentially hydrogen. Shawinigan black is used extensively in rubber and plastic formulations.

Excelsior is channel black manufactured by the Columbian Carbon Company. Excelsior has an average particle size of about 300 Å and a volatile content of 5%.

The one anthracite used in this study is a St. Nicholas anthracite which was ground and passed through a 325 mesh screen. This

* Recently the authors became aware of an error in the scattered intensity[15]. Using the nickel–cobalt balanced filter adjacent to the counter resulted in fluorescent scattering from the cobalt filter entering the counter. This spurious scattering resulted in a maximum error of about 7 per cent in the intensity measurement at the very small angles, but no attempt was made to correct for this relatively constant error. Placing the balanced filter before the carbon specimen would eliminate fluorescent scattering.

[15] Private communication from M. Short, The Pennsylvania State University, 1958.

sample contained 8% mineral matter and 3% volatile matter.

Graphites used in this study consisted of a National Carbon spectroscopic graphite SP-1, a 2 μ natural Ceylon graphite, and a Ceylon graphite ground to a very small particle size. The latter two samples were supplied by the Joseph Dixon Crucible Co. The volatile matter of all the graphites is extremely low. The mineral matter in the graphites ranges from nil in SP-1 to about 2% in the 2 μ and highly ground Ceylon graphite. In addition, the highly ground Ceylon graphite sample was contaminated with about 1.8% iron from the ball mill during the fine grinding operation.

As has been noted previously[17], the decrease in interlayer spacing of carbon blacks upon heat treatment is related qualitatively to the particle size of the black—the larger the particle size the greater the decrease in interlayer spacing. The effect of heat treatment on the crystallographic parameters of anthracite and finely ground Ceylon graphite have been previously discussed[20,21].

The effect of oxidation in a flowing stream of atmospheric pressure air to 5, 12, and 22% weight loss before and after heat treatment of Spheron 6 was studied and the results presented in Table III. Comparing the results with the unoxidized Spheron 6 in Table II for heat treatment temperatures of 1600 and 2500°C, it is seen that oxidation has a negligible effect on the crystallographic parameters. This is in sharp contrast to the marked effect of oxidation on the helium

TABLE I

Summary of Crystallographic Parameters for Raw Carbons

Sample	d(002), Å.	L_c, Å.	L_a, Å.
Carbolac 1	3.65	7	19[16]
Carbolac 2	3.65	7	—
Monarch 71	3.74	9	—
Mogul A	3.65	10	—
Excelsior	3.71	12	—
Spheron 6	3.67	11	23[17]
Vulcan 3	3.66	10	24[17]
Shawinigan	3.62	12	22[18]
Sterling S	3.61	12	26[17]
Sterling FT	3.60	16	28[19]
Sterling MT	3.60	15	—
Anthracite	3.56	17	—
Spectroscopic graphite	3.354	∞	∞
2μ Ceylon graphite	3.354	∞	∞
Finely ground Ceylon graphite	3.63	10	52

III. RESULTS

A. *Crystallite Parameters of Carbons*

Table I presents interlayer spacing and crystallite size data for the carbons studied. The carbon blacks are arranged in order of increasing particle size. The (10) diffraction peak for most of the raw carbons was weak, making the determination of L_a uncertain. Thus, L_a values reported are taken from the literature.

Table II summarizes the changes in crystallographic properties of the carbons following heat treatment at various temperatures.

[16] W. R. Smith, *Encyclopedia of Chemical Technology*, Interscience, New York, Vol. 3., pp. 34–65 (1949).

[17] W. D. Schaeffer, W. R. Smith and M. H. Polley, *Ind. Eng. Chem.* **45**, 1721 (1953).

[18] L. E. Alexander and E. C. Sommer, *J. Phys. Chem.* **60**, 1646 (1956).

[19] W. R. Smith and M. H. Polley, *ibid.*, p. 689.

[20] C. R. Kinney, M. G. Boobar and C. C. Wright, *Industr. Engng. Chem.*, **50**, 27 (1958).

[21] P. L. Walker, Jr. and S. B. Seeley, *Proc. Third Carbon Conf.* Pergamon Press (1959), p. 481.

TABLE II

Summary of Crystallographic Parameters for Heat Treated Carbons

Sample	Heat treatment Temperature, °C	$d(002)$, Å	L_c, Å	L_a, Å
Carbolac 1	2800	3.62	16	55
Carbolac 2	1600	3.71	9	44
Carbolac 2	2500	3.58	20	60
Monarch 71	2800	3.55	24	68
Mogul A	2800	3.47	48	80
Excelsior	513	3.72	12	—
Excelsior	1000	3.72	13	43
Excelsior	1643	3.52	34	79
Excelsior	2500	3.48	36	84
Spheron 6	1600	3.52	21	60
Spheron 6	2500	3.48	46	80
Vulcan 3	2700	3.44	41	60
Shawinigan	2800	3.44	60	50
Sterling S	2700	3.41	114	150
Sterling FT	1000	3.58	16	47
Sterling FT	1500	3.47	37	69
Sterling FT	2700	3.39	141	144
Sterling MT	2800	3.36	148	184
Anthracite	2800	3.356	137	174
Finely ground Ceylon graphite	1600	3.60	13	53
	2500	3.40	70	60

TABLE III

Summary of Crystallographic Parameters for Spheron 6 Oxidized Before and After Heat Treatment

Heat treatment, Temperature, °C	Oxidation, %	$d(002)$, Å	L_c, Å	L_a, Å
		Oxidized before heat treatment		
1600	5	3.52	23	64
1600	12	3.54	22	64
1600	22	3.53	20	58
2500	5	3.45	41	80
2500	12	3.49	38	84
2500	22	3.48	36	80
		Oxidized after heat treatment		
1600	5	3.52	24	66
1600	12	3.49	26	64
1600	22	3.50	25	63
2500	5	3.46	43	87
2500	12	3.45	43	81
2500	22	3.45	43	88

density of Spheron 6 under similar treatment conditions, as will be discussed shortly.

B. *Densities and Porosities of Carbons*

Helium, X-ray, and particle (apparent) densities have been determined on some of the raw, oxidized, and heat treated carbons. From these densities, total porosities and porosities closed to helium have been calculated using the equations:

$$\text{Total porosity } (\%) = 100(1 - \rho_{\text{part}}/\rho_{\text{X-ray}}) \quad (1)$$

$$\text{Closed porosity } (\%) = 100(1 - \rho_{\text{He}}/\rho_{\text{X-ray}}) \quad (2)$$

For carbon blacks of smaller particle size

than Spheron 6 and the finely ground Ceylon graphite, the mercury porosimeter could not be taken to sufficiently high pressures to fill the voids between particles; and therefore, their apparent densities could not be determined directly. However, for these carbons sufficient pressure was available to estimate a maximum packing density; and assuming that the packing porosity of the blacks was about 30 per cent[22], particle densities were calculated.

The densities and porosities for the raw carbons are presented in Table IV. The densities for anthracite and the Ceylon graphites have been corrected in each case for mineral matter. For the finely ground Ceylon graphite, an added correction has been made for the presence of iron introduced during grinding. Some observations from Table IV are as follows:

1. The channel blacks have large total porosities, with the majority of the porosity open to helium.

2. The furnace and thermal blacks vary in properties. Vulcan 3, an oil furnace black, has similar porosity characteristics to the channel blacks. The other furnace and thermal blacks studied also have substantial total porosities, but the percentage of the total porosity closed to helium becomes significant. In the most extreme case, Sterling MT, the closed porosity constitutes 92% of the total porosity.

3. The spectroscopic graphite has a negligible porosity.

TABLE IV

Densities and Porosities for Raw Carbons

Sample	Density, g/cm³			Particle porosity, %	
	X-ray	Helium	Particle	Closed	Total
Carbolac 1	2.08	2.02	1.43	3	32
Carbolac 2	2.08	2.00	1.20	4	42
Monarch 71	2.04	2.04	1.33	0	35
Mogul A	2.08	2.06	1.41	1	33
Excelsior	2.05	2.01	1.38	2	33
Spheron 6	2.07	1.94	1.35	6	35
Vulcan 3	2.08	2.06	1.31	1	37
Shawinigan	2.09	1.87	1.42	11	32
Sterling S	2.10	1.93	1.64	8	22
Sterling FT	2.11	1.88	1.66	11	21
Sterling MT	2.11	1.84	1.81	13	14
Anthracite	2.13	1.91	1.51	10	29
Spectroscopic graphite	2.26	2.26	2.23	0	1
2 μ Ceylon graphite	2.26	2.17	2.08	3	8
Finely ground Ceylon graphite	2.09	2.09	1.55	0	26

4. The anthracite has a substantial total and closed porosity.

The densities and porosities for the heat treated carbons are presented in Table V. Marked differences in the effect of heat treatment on the carbons are noted, as summarized below:

1. For the channel blacks, there is a decrease in total porosity accompanied by a substantial increase in the closed porosity. Whereas for the raw channel blacks the closed porosity is in all cases less than 6%, for the channel blacks heated to 2500°C or above the closed porosities range from 12 to 28%.

2. The effect of heat treatment on the change of porosities for Vulcan 3 and Shawinigan is qualitatively similar to that found for the channel blacks.

3. For the three Sterling blacks, both the

[22] J. M. Dallavalle, *Micromeritics*, Pitman, New York (1948), p. 127.

TABLE V

Densities and Porosities for Heat Treated Carbons

Sample	Heat treatment temperature °C	Density, g/cm³ X-ray	Helium	Particle	Particle porosity, % Closed	Total
Carbolac 1	2800	2.10	1.52	1.51	28	28
Carbolac 2	1600	2.05	1.77	—	14	—
Carbolac 2	2500	2.12	1.56	1.30	27	39
Monarch 71	2800	2.14	1.73	1.67	19	22
Mogul A	2800	2.19	1.85	—	16	—
Excelsior	513	2.04	2.01	—	1	—
Excelsior	1000	2.04	(2.09)	—	—	—
Excelsior	1643	2.16	1.89	—	10	—
Excelsior	2500	2.18	1.89	1.75	14	20
Spheron 6	1600	2.16	1.90	1.64	12	24
Spheron 6	2500	2.18	1.92	1.72	12	21
Vulcan 3	2700	2.12	1.93	1.51	13	32
Shawinigan	2800	2.21	1.80	1.66	17	25
Sterling S	2700	2.22	2.06	1.75	7	21
Sterling FT	1000	2.13	1.89	1.71	12	20
Sterling FT	1500	2.19	2.04	1.85	7	16
Sterling FT	2700	2.24	2.16	2.05	3	8
Sterling MT	2800	2.25	2.13	2.12	5	6
Anthracite	2800	2.26	2.00	1.91	11	15
Finely ground Ceylon graphite	1600	2.11	2.09	—	1	—
	2500	2.23	1.80	1.69	20	24

TABLE VI

Helium and X-ray Densities and Closed Porosities for Spheron 6 Oxidized Before and After Heat Treatment

Heat treatment temperature, °C	Oxidation % Burn-off	Densities, g/cm³ X-ray	Helium	Closed porosity, %
None	None	2.07	1.94	6
None	5	2.07	1.97	5
None	12	2.07	2.00	4
None	22	2.07	1.95	6
	Oxidized before heat treatment			
1600	5	2.16	1.78	18
1600	12	2.15	1.74	19
1600	22	2.14	1.68	22
2500	5	2.20	1.78	19
2500	12	2.18	1.77	19
2500	22	2.18	1.64	25
	Oxidized after heat treatment			
1600	5	2.16	1.98	8
1600	12	2.18	2.04	7
1600	22	2.17	1.99	8
2500	5	2.20	1.89	14
2500	12	2.20	1.98	10
2500	22	2.20	1.98	10

total and closed porosities are reduced upon heat treatment.

4. Heat treatment to 2800°C decreases the total porosity of the anthracite but has little effect on the closed porosity.

5. Heat treatment of finely ground Ceylon graphite to 2500°C greatly increases the closed porosity but has little effect on the total porosity.

The effect of oxidation of Spheron 6 before and after heat treatment (as previously described) on closed porosities has also been investigated and the results presented in Table VI. Any changes in the amount of closed porosity is a result of a change in helium density, since the X-ray densities are changed an insignificant amount. Oxidation of Spheron 6 prior to heat treatment to 1600 and 2500°C is seen to increase markedly the resulting closed porosity over that of the unoxidized Spheron 6 heat treated to the same temperatures. Further, the amount of closed porosity increases with increase in extent of oxidation before heat treatment. On the other hand, oxidation of Spheron 6 following heat treatment to 1600°C is seen to result in a decrease in closed porosity over that of the unoxidized samples heat treated to this temperature. Oxidation of Spheron 6 following heat treatment to 2500°C has a small effect on closed porosity.

C. *Small-Angle Scattering Results*

1. *Correlation of small-angle scattering intensities with BET surface areas.* Debye *et al.*[23] and Porod[24] have developed theories which show that specific surface areas can be determined when the intensity of scattering of X-rays from inhomogeneous solids vary inversely as the fourth power of the scattering angle. Van Nordstrand and co-workers[25,26] have used this concept to determine the relative surface areas of a series of cracking catalysts. They[26] find a linear relationship between intensity of X-ray scattering at 0.05 rad and BET surface area for a series of silica–alumina cracking catalysts.

It was of interest to explore the possibility of a similar correlation for a series of raw and graphitized carbon blacks. First, some typical log I vs. log ϵ curves are presented in

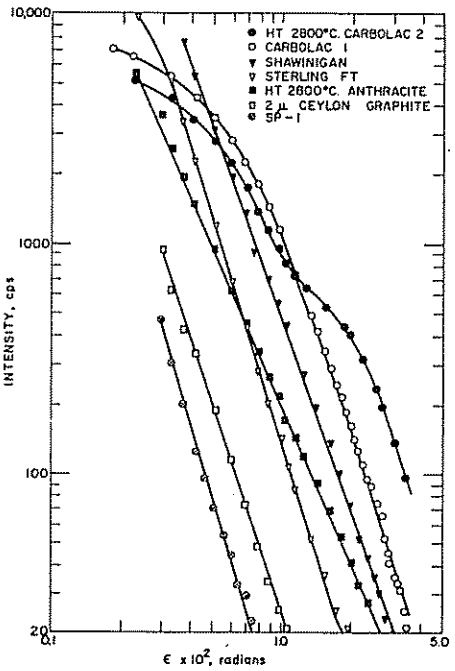

FIG. 1. Typical log I vs. log ϵ plots for carbons.

Fig. 1 to illustrate several qualitative features of the small-angle scattering plots, where $\epsilon = 2\theta$ in radians. The plots are seen to be linear over a wide range of angle, with a marked increase in scattering intensity in going from a low surface area graphite (SP-1) to a high surface area carbon black (Carbolac 1). The only sample showing a slope much

---

[23] P. Debye, H. R. Anderson, Jr. and H. Brumberger, *J. Appl. Phys.* **28**, 679 (1957).

[24] G. Porod, *Kolloid-Z.* **124**, 83 (1951).

[25] R. A. Van Nordstrand and K. M. Hack, *Small Angle X-ray Scattering of Silica and Alumina Gels*, Presented at the Catalysis Club, Chicago (May, 1953).

[26] R. A. Van Nordstrand and M. F. L. Johnson, *Small Angle X-ray Scattering of Cracking Catalyst Comparison with Adsorption Isotherms*, Presented at the Pittsburgh Conference on X-ray and Electron Diffraction (November, 1954).

less than 4 is the heat treated anthracite. According to Van Nordstrand and Johnson[26], a low slope can be associated with a solid containing very fine pores. Anthracite is known to be a molecular sieve material[27]. The scattering curves for raw Carbolac 1 and heat treated Carbolac 2 are seen to bend over sharply at lower angles; this is characteristic for materials of small particle size[25], such as Kuroda[28] at comparable angles. On the other hand, it is seen that above 100 m^2/g the relationship between the scattered intensities and BET surface areas is essentially independent of heat treatment temperature for the blacks. For the raw carbon blacks which have areas greater than 200 m^2/g (with the surface area change primarily a result of change in internal porosity) it is seen that the

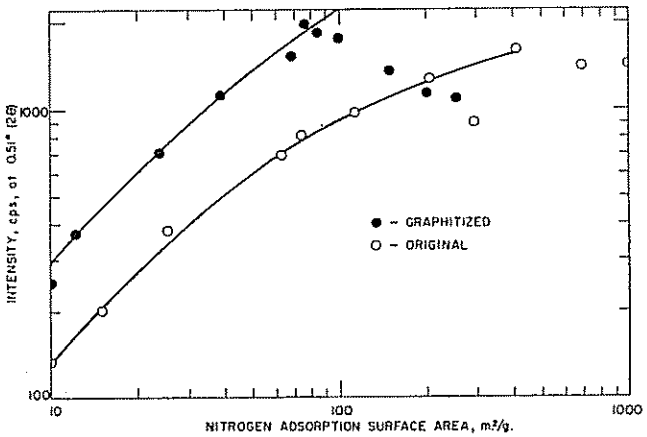

FIG. 2. Correlation between X-ray intensity and nitrogen adsorption surface area for original and graphitized carbon blacks.

these two channel blacks. For the heat treated-Carbolac 2 sample, there is a sharp break in the scattering curve at about 1 rad. This is interpreted as indicative of some long range ordering and will be discussed in more detail later.

Figure 2 presents a correlation between scattering intensity at 0.51° (2θ) and BET surface area for the series of raw and graphitized carbon blacks. First, it is evident for surface areas up to 100 m^2/g that the scattered intensity is considerably greater for the graphitized carbon blacks than for the raw carbon blacks at equal surface areas. A gradual increase in scattering intensity with increase in heat treatment temperature of a carbon black has been noted by Akamatu and scattered intensities have reached a maximum and essentially constant value. This suggests that at the particular scattering angle selected for this correlation, the scattered intensity is primarily produced by discontinuities between particles (or a function of particle size). Figure 3, where scattered intensity is plotted against geometric surface area (the areas calculated from average particle size data supplied by the manufacturers), appears to confirm this reasoning.

2. *Correlation distance.* According to Debye and co-workers[23], small angle scattering data on an inhomogeneous solid can be used to determine an average correlation distance (a_1) for the solid, where a_1 is a length measuring the extent of inhomogeneities. From a

[27] P. L. Walker, Jr. and Irwin Geller, *Nature, Lond.* **178,** 1001 (1956).

[28] H. Akamatu and H. Kuroda, *Proc. Third Carbon Conf.* Pergamon Press (1959), p. 381.

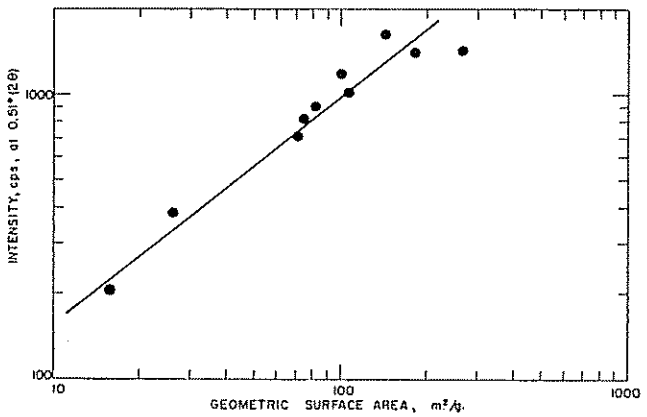

FIG. 3 Correlation between X-ray intensity and geometric surface area for original carbon blacks.

graphical plot of intensity$^{-1/2}$ vs. $(\epsilon)^2$ (called slope-intercept plots), the relation

$$a_1 = \frac{\lambda}{2\pi}\left(\frac{\text{slope}}{\text{intercept}}\right)^{1/2} \qquad (3)$$

is used to determine the inhomogeneity length.

Figure 4–6 present some slope-intercept plots for raw and heat-treated carbons, ranging from samples of low to high scattering intensities. These curves usually may be divided into two different regions of importance in determining correlation distances: (1) a long, linear region of constant slope is found where the scattered intensity is inversely proportional to the fourth power of the scattering angle. This linear portion of the curve is used to evaluate a_1; (2) a region of constantly changing slope at the smaller angles is found. A second correlation distance can be calculated from this region, referring to larger inhomogeneous discontinuities. Qualitative observations to be made from Figs. 4–6 are:

1. Ceylon and SP-1 graphites (having the lowest surface areas) have the steepest slope.

2. For the carbon blacks there is a decrease in slope with decrease in particle size.

3. For the carbon blacks, there is a decrease in slope with increase in heat treatment temperature. (Samples of Excelsior and Sterling FT carbon blacks were heat treated at a series of temperatures up to 2700°C and showed a progressive decrease in slope with increase in heat treatment temperature. These plots are not shown.)

4. For samples of Carbolac 1 and Monarch 71 heat treated to 2800°C, there is a slight hump in the curve at small angles. This suggests some long-range ordering, in a similar fashion to that suggested previously for graphitized Carbolac 2.

The effect of oxidation of Spheron 6 before and after heat treatment at different temperatures on the slope-intercept plots is shown in Figs. 7 and 8. Oxidation before or after heat treatment results in an increase in scattering (decrease in slope). In some cases, a sufficient region of linearity is not obtained to make possible the calculation of a correlation distance.

As mentioned, a second correlation distance can be calculated when the slope-intercept plots deviate from linearity at small angles. According to Debye and co-workers[23], a_2 is calculated from the slope of a plot of the log of the intensity difference between the curved and linear portion of the slope-intercept plots and ϵ^2, using the equation

$$a_2 = \frac{\lambda}{\pi}(2.3 \times \text{slope})^{1/2} \qquad (4)$$

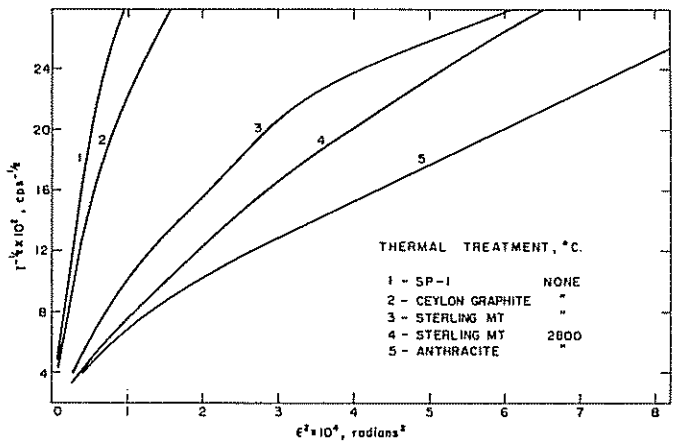

FIG. 4. Slope-intercept plots for carbons of low scattering.

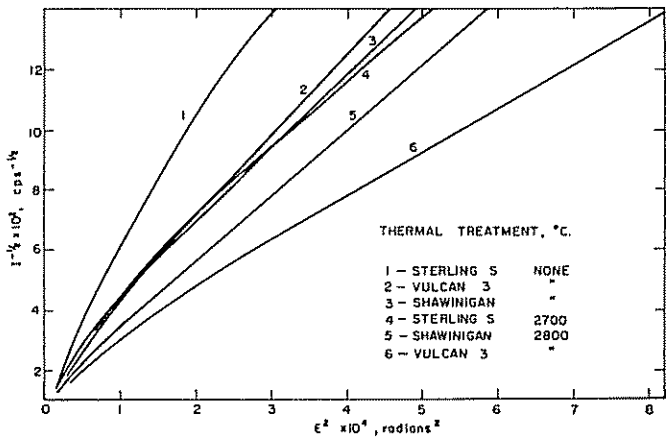

FIG. 5. Slope-intercept plots for carbons of intermediate scattering.

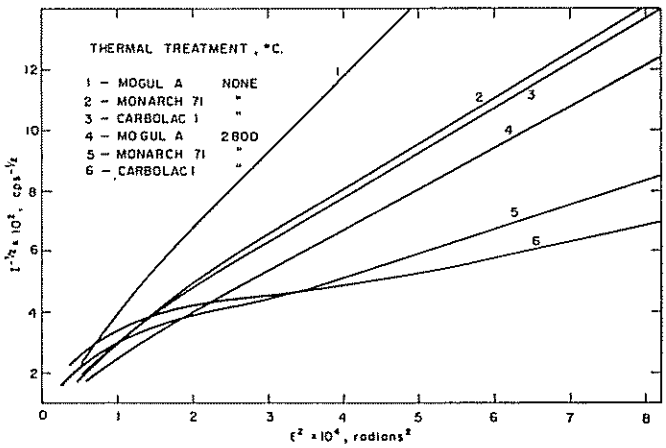

FIG. 6. Slope-intercept plots for carbons of high scattering.

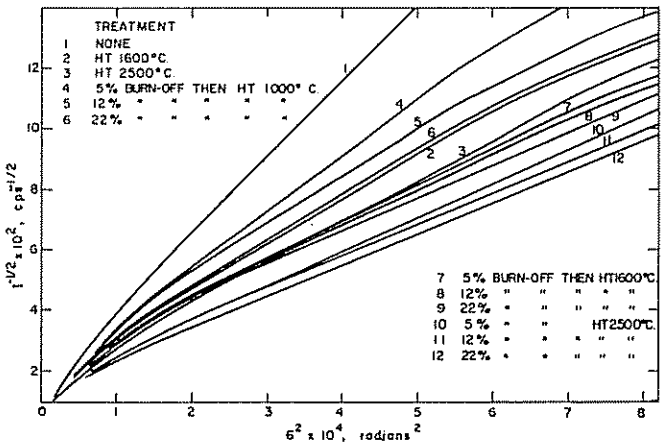

FIG. 7. Slope-intercept plot for original and heat treated Spheron 6 and for samples oxidized before heat treatment.

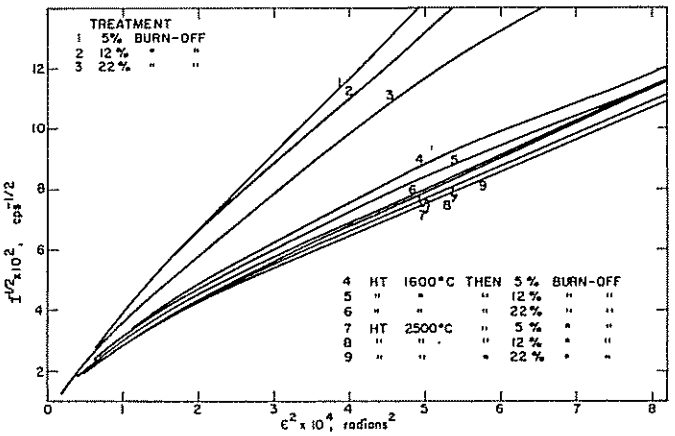

FIG. 8. Slope-intercept plots for oxidized original Spheron 6 and for samples oxidized after heat treatment.

Figure 9 presents a typical plot for raw and heat treated Excelsior. It is seen for the heat treated sample that there is some tailing up at very small angles. The calculation of a third correlation distance, a_3, appears practical and is discussed elsewhere[14].

The average correlation distances, a_1 and a_2, for some of the raw and heat treated samples are given in Table VII. Because of the hump in the slope-intercept plots for heat treated Carbolac 1 and 2, their correlation distances were not calculated. It is seen from Table VII that there is no marked change in a_1 upon graphitization, even though some decrease is evident for three of the four carbon blacks studied.

3. *Surface areas of carbons.* According to Debye and co-workers[23], the specific surface area of an inhomogeneous solid can be calculated by the equation

$$S/V = \frac{4\phi(1-\phi)}{a_1} \qquad (5)$$

where $\phi = 1 - (\rho_a/\rho_t)$ and ρ_a and ρ_t are the

particle (apparent) and true (X-ray) density of the solid, respteeively.* The area per unit

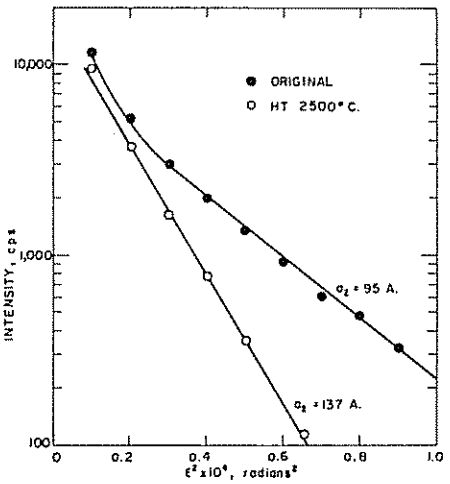

FIG. 9. Evaluation of a_2 for original and heat treated Excelsior.

volume (S/V) can be converted to area per unit mass from knowledge of ρ_a. Surface areas calculated, where possible, from correlation distances for raw and heat treated carbons are compared with BET surface areas in Tables VIII and IX. For the raw carbon blacks, electron microscope surface areas are also given. These results will be discussed later in the paper.

4. *Correlation functions.* Debye and co-workers[23] and Gunn[29] have discussed the use of a characteristic correlation function to interpret small-angle scattering data. This function, $\gamma(r)$, represents an average value of correlations in electron variations throughout regions of the porous solid separated by a specific distance. The function can be expressed as

$$r\gamma(r) = C\int KI(K)\sin Kr\,dK \qquad (6)$$

* Strictly speaking, when more than one correlation distance is found for a solid, the calculation for X-ray surface area should take this into account. However, Debye and co-workers[23] find that areas calculated for cokes, ignoring the contribution of a_2, agree within 5% with those calculated including this term. Since the uncertainty in the X-ray surface areas is greater than 5%, only a_1 will be used in this calculation.

where C is a constant, $I(K)$ is the observed intensity of scattering as a function of K, and

TABLE VII
Average Correlation Distances for Some Raw and Heat Treated Carbons

Sample	a_1, Å	a_2, Å
Raw		
Carbolac 1	23	83
Carbolac 2	17	75
Excelsior	26	95
Spheron 6	31	95
Finely ground Ceylon graphite	19	115
Anthracite	20	—
*Heat Treated**		
Carbolac 1	N	—
Carbolac 2	N	—
Excelsior	22	137
Spheron 6	31	97
Finely ground Ceylon graphite	15	80
Anthracite	17	94

N not obtainable from slope-intercept plots.
* Heat treated to 2500°C or above (see Table V for highest heat-treatment temperature).

$K = (4\pi \sin\theta)/\lambda$. A method, similar to that suggested by Gunn,[29] was employed for the evaluation of $\gamma(r)$ from small angle scattering data. The data were programmed and $\gamma(r)$ evaluated by means of the Pennstae Electronic Computer, as described in detail elsewhere[14].

Figure 10 presents correlation function plots for original and heat treated Spheron 6 specimens. The presence of an increasing number of smaller inhomogeneities with increasing heat treatment temperature is apparent. For example, at $\gamma(r) = 0.5$, the correlation distances are 43 and 32 Å for the original and heat treated 2500°C samples. Alternatively, it is seen that $\gamma(r)$ values for the heat treated samples are lower than for the original Spheron 6 at all r values. For example, at $r = 100$ Å the probability of greater correlation distances is 20% for the original material and 10% for the material

[29] E. L. Gunn, *J. Phys. Chem.* **62,** 928 (1958).

TABLE VIII
Comparison of Specific Surface Areas for Raw Specimens

Sample	Average correlation distance, a_1, Å	Surface area, m^2/g		
		X-Ray	BET	Elec. Mic.
Carbolac 1	23	265	980	264
Carbolac 2	17	480	715	178
Monarch 71	21	325	420	145
Mogul A	32	196	293	82
Excelsior	26	246	210	100
Spheron 6	31	219	114	106
Vulcan 3	29	243	74	77
Shawinigan	26	236	64	70
Sterling S	N	—	26	26
Sterling FT	N	—	15	16
Sterling MT	N	—	9	6
Anthracite	20	275	46	—
2μ Ceylon graphite	N	—	10	—
Finely ground Ceylon graphite	19	262	58	—

N Not obtainable.

heat treated to 2500°C. The probability referred to is for the two ends of r to be in different electron density environments.

Figure 11 presents correlation function plots for original and heat treated Carbolac 2. The correlation function at all values of r is observed to increase upon heat treatment at 1600°C and then to decrease upon heat treatment to 2500°C. The correlation function for Carbolac 2 heat-treated to 2500°C is seen to decrease sharply to an r value of 50 Å, then to show a slight increase before approaching

TABLE IX
Comparison of Specific Surface Areas for Heat Treated Specimens

Sample	Heat treatment temperature, °C	Average correlation distance, a_1, Å	Surface area, m^2/g	
			X-ray	BET
Carbolac 1	2800	N	—	251
Carbolac 2	1600	N	—	328
Carbolac 2	2500	N	—	202
Monarch 71	2800	N	—	149
Mogul A	2800	24	—	86
Excelsior	513	26	—	213
Excelsior	1000	N	—	245
Excelsior	1643	22	—	121
Excelsior	2500	22	169	98
Spheron 6	1600	N	—	84
Spheron 6	2500	N	—	79
Vulcan 3	2700	20	287	68
Shawinigan	2800	32	140	39
Sterling S	2700	N	—	34
Sterling FT	1000	N	—	13
Sterling FT	1500	N	—	13
Sterling FT	2700	N	—	12
Sterling MT	2800	N	—	10
Anthracite	2800	17	160	5
Finely ground Ceylon graphite	1600	15	—	513
	2500	15	289	128

N Not obtainable from slope-intercept plot.

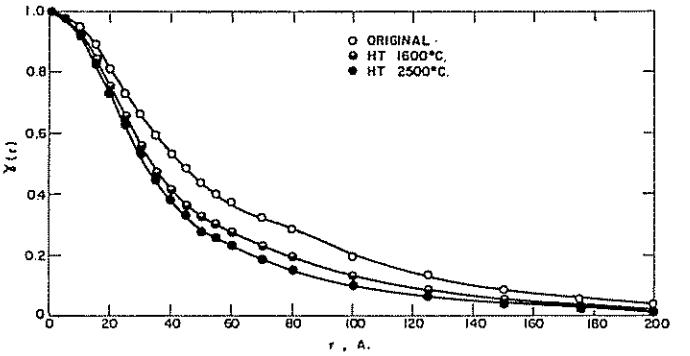

FIG. 10. Correlation function plots for original and heat-treated Spheron 6.

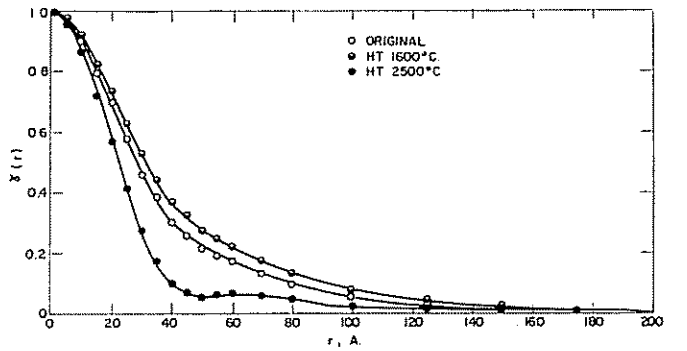

FIG. 11. Correlation function plots for original and heat treated Carbolac 2.

zero for large values of r. This hump in the curve, with a maximum at *ca.* 60 Å, indicates some long-range ordering, as previously suggested from Fig. 1.

Figure 12 presents correlation function plots for Spheron 6 oxidized to 5, 12 and 22% burn-off. The correlation function decreases with increased oxidation for all r values. However, the correlation function plots for the original Spheron 6 and the sample oxidized to 5% burn-off are essentially identical.

Debye *et al.*[23], for simplicity, have expressed $\gamma(r)$ as the sum of two exponentials in the form

$$\gamma(r) = fe^{-r/a_1} + (1 - f)\exp(-r^2/a_2^2) \quad (7)$$

where a_1 and a_2 are correlation distances, as previously discussed, and f is given by

$$f = \frac{A_1}{A_1 + (8/\sqrt{\pi})(a_1/a_2)^3 A_2} \quad (8)$$

where A_1 and A_2 are constants. A_1 and A_2 (and, therefore, f) can be calculated[23].

It was of interest to compare a correlation function curve calculated from Debye's simplified model (Eq. 7) with that calculated using Eq. (6). This comparison is made in Fig. 13 for raw Excelsior taking $a_1 = 26$ Å and $a_2 = 95$ Å. The value of $f = 0.73$ has been calculated in the suggested manner. It is seen from Fig. 13 that for low values of r the calculated curve deviates from the shape of the experimental (rigorous) curve but that for larger values of r the two curves parallel each other. By trial and error, a better fit between the experimental and calculated curves is obtained for $f = 0.64$. For low values of r, however, there is still some deviation between the two curves. The important conclusion to draw from this comparison is that the Debye model, assuming $\gamma(r)$ to be the sum of two exponentials, is only

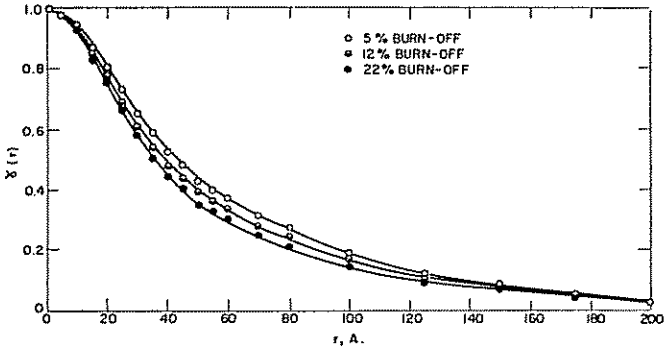

FIG. 12. Correlation function plots for oxidized Spheron 6.

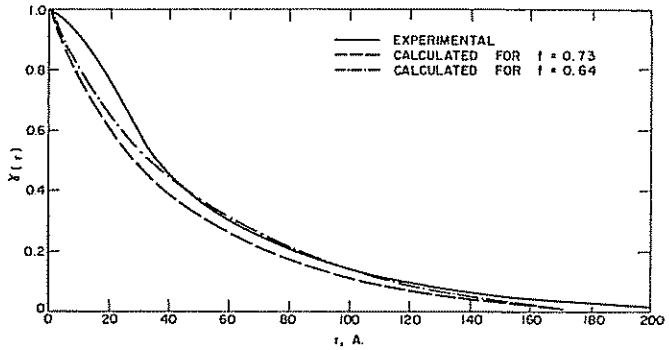

FIG. 13. Comparison of an experimental correlation function curve $[r\gamma(r) = C\int KI(K)\sin Kr\,dK]$ with the correlation function curves calculated from the Debye model $[\gamma(r) = \exp(-r/a_1) + (1-f)\exp(-r^2/a_2^2)]$ for $a_1 = 26$ Å and $a_2 = 95$ Å.

an approximation. For larger values of r, this approximation is rather good, but for low values of r (r less than *ca.* 40 Å) this approximation does not completely describe $\gamma(r)$.

IV. DISCUSSION

Carbons whose properties are affected to widely different extents by heat treatment and oxidation have been studied in this work. On the basis of their change in properties, they can be classified into two main groups:

Group one: These carbons show a large decrease in helium density and BET surface area and an increase in particle density upon heat treatment, indicating the production of an extensive closed pore system.

Group two: These carbons show an increase in helium and particle densities and a slight decrease in BET surface area upon heat treatment, indicating the development of a dense, compacted particle structure.

Carbons most clearly showing the properties of Group one include the small particle size, high internal (open) surface area channel blacks and the finely ground Ceylon graphite. Carbons most clearly showing the properties of Group two include the large particle size, low internal (open) surface area thermal blacks.

A quantitative explanation for the changes in physical properties of the carbons with heat treatment is difficult. However, for the carbon blacks which have been studied, the extent of oxidation of the material before heat

treatment appears of considerable importance. This is brought out by the results on Spheron 6, which was oxidized to varying burn-offs before heat treatment. For example, 5% oxidation of raw Spheron 6 increases the helium density from only 1.94 to 1.97 g/cm^3. However, on heat treatment to 2500°C, the original Spheron 6 has a helium density of 1.92 g/cm^3, whereas the Spheron 6 previously oxidized to 5 per cent weight loss has a density of only 1.78 g/cm^3. At the same time, it is recalled that prior oxidation has a negligible effect on the change of the crystallographic parameters of Spheron 6 upon heat treatment to 2500°C.

The highly porous channel blacks (which show a large decrease in helium density upon heat treatment to 2500°C as does the oxidized Spheron 6) have been strongly oxidized during their formation. On the other hand, the thermal blacks have not been oxidized significantly during their formation and show an increase in helium density upon heat treatment to *ca.* 2700°C. It is known that oxidation of thermal blacks prior to heat treatment greatly increases their internal porosity[30] and it would be predicted that their helium densities would decrease upon heat treatment following pre-oxidation.

Vulcan 3 is an outstanding exception to the ideas just discussed. This oil furnace black has a negligible internal surface area, indicating little oxidation during its production. However, upon heat treatment to 2700°C, it shows a large decrease in helium density from 2.06 to 1.93 g/cm^3, a behavior similar to that of the highly porous channel blacks. It is suggested that the production of Vulcan 3 from liquid hydrocarbons, in comparison to gaseous hydrocarbons (for example, Sterling S is a gas furnace black) may be responsible for the high helium density of the raw black. However, the reason for the decrease in density upon graphitization is not clear.

It is of interest to explore the possibilities of using small angle X-ray scattering to obtain additional data on the physical structure of carbons, as well as to explore the opportunities in using this technique to more easily and quickly obtain data which is now being obtained by some other technique. Points of particular interest which were explored were:

1. Use of scattering intensities at a fixed angle to predict relative geometric and BET surface areas of carbons.

2. Use of scattering data and apparent densities of carbons to calculate quantitative surface areas for the interior of the particle.

3. Relation between correlation distance calculated from scattering data and crystallite size calculated from diffraction line broadening.

Considering point one, it is found for the experimental conditions employed in this research, that the scattered intensity at 0.51° (2θ) can be used as a good qualitative indication of the geometric surface areas of raw carbon blacks. The carbon blacks studied cover the complete range of commercial materials from high porosity, small particle sized channel blacks to low porosity, large particle sized thermal blacks. Unlike the findings of Van Nordstrand and co-workers[25,26], a general correlation was not found, however, between scattered intensity at a fixed angle and BET surface area. This is probably explained by two reasons. First, Van Nordstrand *et al.*, apparently because they were successful in obtaining reproducible scattering intensities down to less than 1 c/sec, were able to correlate their BET surface area results with scattered intensities at a much higher angle (*ca.* 5°(2θ)) than was possible in the present work. At this higher angle, the smaller sized pores, which are apparently contributing strongly to the BET surface area of their catalysts, are scattering strongly. Secondly, a correlation between scattered intensity and BET surface area would not be expected if the solids contained a significant and varying amount of porosity

[30] W. R. Smith and M. H. Polley, *J. Phys. Chem.* **60**, 689 (1956).

which is closed to the adsorbate used to measure BET area. This is the case for the carbon blacks. Many of the raw blacks have porosity (surface area) impervious to helium at room temperature and obviously, therefore, impervious to nitrogen at 77°K. Apparently, for the catalysts studied by Van Nordstrand *et al.* there was either a negligible closed surface area or a constant percentage of closed surface area as the total area changed.

Considering point two, there was interest in using scattering data to determine the total internal surface area of carbons—both the area open to the adsorbate measuring the BET surface and area closed to the adsorbate. That is, the area of a porous carbon can be considered to be composed of the sum of the geometric surface area, given by the particle size of the carbon; the open internal surface area; and closed internal surface area. The first two area contributions can be determined in a routine manner. From a particle size distribution obtained from electron micrographs, the geometric area is calculated. The difference between the BET area and the geometric surface area gives the open internal surface area. Therefore, if from scattering data the total internal surface area can be calculated, the area which is closed can also be calculated by subtracting the open internal surface area contribution.

For it to be possible to calculate the total internal surface area of carbons, it is first necessary that the slope-intercept Debye-plots are not affected by the external surface area of the solid. For large particle sized solids with small internal pores (open and closed) this is undoubtedly the case. However, in the present work, where some of the carbon blacks are of quite small particle size, it is not clear to what extent the inhomogeneities between particles can be contributing to scattering in the range where the slope-intercept plots obey the fourth power region. It is, therefore, difficult to interpret the meaning of X-ray surface areas as reported in Tables VIII and IX.

A further difficulty exists in determining quantitative X-ray surface areas, particularly for small particle sized solids. The particle density of the solid must be known, as seen in Eq. 5. The determination of this density can be as difficult as the determination of low angle scattering data and perhaps requires more elaborate equipment. In the present work, the particle density was determined by filling the voids between the particles with mercury, using a conventional mercury porosimeter apparatus. For the smaller size carbon blacks, the apparatus could not be taken to sufficiently high pressures to fill all the voidage between particles; and a particle density had to be estimated. The authors feel that more recognition should be given to the need of having accurate particle density data by workers in this field.

In line with the discussion, the X-ray, BET, and geometric surface area data presented in Table VIII can be considered briefly. First, for the high surface area channel black samples the results are confusing. For Carbolac 1, the open internal surface area is calculated to be 718 m^2/g and yet the X-ray surface area is only 265 m^2/g. Perhaps uncertainty in the particle density of Carbolac 1 accounts for this discrepancy. For Carbolac 2, results appear more reasonable. The open internal surface area is calculated to be 537 m^2/g in comparison with the X-ray surface area of 480 m^2/g. This would suggest that raw Carbolac 2 has a negligible closed internal surface area. This is in line with the small closed porosity calculated for this material, as seen in Table IV. Results for raw Monarch 71 and Mogul A likewise appear to be reasonable. For Shawinigan black, it is concluded that the open internal surface area is negligible but that the closed internal surface area is substantial (at least 166 m^2/g). It can be reasoned that this large closed internal area is in line with the large closed porosity of Shawinigan black of 11%.

It should be noted that Debye and coworkers[23] also had some difficulty relating

X-ray surface area to BET surface area for a relatively large particle size coke sample. That is, they report a BET area of 400 m^2/g and an X-ray area of only 245 m^2/g.

Considering point three, there has been considerable interest in relating the correlation distance calculated from the slope-intercept plots to some other, measured physical parameter of solids. In essence, as described by Guinier, *et al.*[31], it is difficult to decide whether the scattering is primarily produced by the size of the grains or crystallites composing the solid or by the size of the voids and pores. Gunn[29] recently found a good qualitative relation between the correlation distance (a_1) for a number of cobaltia-molybdena-alumina catalysts and the most frequent pore size in the catalyst calculated from the desorption branch of the isotherm for the catalyst. Unfortunately, no desorption isotherms nor complete adsorption isotherms are available for the carbons studied to enable the calculation of an average pore size to be made. At least it appears certain that the correlation distances obtained are not related to the average crystallite size of the carbon black. For example, for Spheron 6 a_1 remains essentially unchanged in going from the raw to the material heated to 2500°C. By comparison, L_c increases from 11 to 46 Å, and L_a increases from 23 to 80 Å.

[31] A. Guinier, G. Fournet, C. B. Walker and K. L. Yudowitch, *Small-Angle Scattering of X-rays*, John Wiley, New York (1955), p. 192.

We wish to thank R. A. Van Nordstrand, P. Debye and H. A. McKinstry for their suggestions in conducting and interpreting the small angle X-ray scattering work. We thank the carbon black companies for supplying samples, Joseph Dixon Crucible Company for fine grinding the graphite, and the Speer Carbon Company for the use of their high temperature resistance furnace. We thank P. Wegner for help in programming the data for the evaluation of the correlation function and the Computer Laboratory staff for carrying out the computations.